Eduquakes

Instrument Response Removal and the 2020 M_{Lg} 3.1 Marlboro, New Jersey, Earthquake

Alexander L. Burky*[1], Jessica C. E. Irving[2], and Frederik J. Simons[1]

Abstract

To better understand earthquakes as a hazard and to better understand the interior structure of the Earth, we often want to measure the physical displacement, velocity, or acceleration at locations on the Earth's surface. To this end, a routine step in an observational seismology workflow is the removal of the instrument response, required to convert the digital counts recorded by a seismometer to physical displacement, velocity, or acceleration. The conceptual framework, which we briefly review for students and researchers of seismology, is that of the seismometer as a linear time-invariant system, which records a convolution of ground motion via a transfer function that gain scales and phase shifts the incoming signal. In practice, numerous software packages are widely used to undo this convolution via deconvolution of the instrument's transfer function. Here, to allow the reader to understand this process, we start by taking a step back to fully explore the choices made during this routine step and the reasons for making them. In addition, we introduce open-source routines in Python and MATLAB as part of our `rflexa` package, which identically reproduce the results of the Seismic Analysis Code, a ubiquitous and trusted reference. The entire workflow is illustrated on data recorded by several instruments on Princeton University campus in Princeton, New Jersey, of the 9 September 2020 magnitude 3.1 earthquake in Marlboro, New Jersey.

Cite this article as Burky, A. L., J. C. E. Irving, and F. J. Simons (2021). Instrument Response Removal and the 2020 M_{Lg} 3.1 Marlboro, New Jersey, Earthquake, *Seismol. Res. Lett.* **XX**, 1–8, doi: 10.1785/0220210118.

Motivation

As seismologists, we are interested in analyzing the ground motion at a particular location, often in the aftermath of an earthquake. To accomplish this task, in modern seismology, large deployments of digital broadband seismometers, accelerometers, and other ground-motion sensors are installed around the globe.

These instruments sense the ground motion at their location, recording a digital version of how they respond mechanically and electrically to the ongoing motion (Bormann, 2012; Havskov and Alguacil, 2016). Hence, a seismogram is a digitized version of the analog quantities of interest, that is, displacement, velocity, or acceleration, convolved with the instrument response, expressed in "counts" (Ringler and Bastien, 2020).

The details of the digitization process (see, e.g., Asch, 2009) are beyond the scope of this article. As scientists, we are typically interested in undoing the effects of the instrument to arrive back at the original physical quantities of interest. To accomplish and understand this process, we require some results from the theory of linear time-invariant systems (see, e.g., Scherbaum, 2001), namely, the properties of convolution and deconvolution, which we briefly review here.

Mathematical Model

The seismometer is modeled as a linear time-invariant system, which takes an input signal $x(t)$ and produces an output signal $y(t)$ according to the convolution integral

$$y(t) = \int_{-\infty}^{\infty} x(t-\tau)h(\tau)d\tau, \tag{1}$$

in which $h(\tau)$ is referred to as the impulse response of the system. In our scenario, the observed, causal output of the seismometer is $y(t)$, the physical ground motion is $x(t)$, and the effect of the conversion is captured by the impulse response, $h(\tau)$. To solve this equation for $x(t)$, we can use a well-known property of convolution integrals: that the convolution of two functions in the time domain amounts to a multiplication of those functions in the frequency (Laplace or Fourier) domain. This allows us to rewrite equation (1) as follows:

1. Department of Geosciences, Princeton University, Princeton, New Jersey, U.S.A., https://orcid.org/0000-0002-0199-1999 (ALB); https://orcid.org/0000-0003-2021-6645 (FJS); 2. School of Earth Sciences, University of Bristol, Bristol, United Kingdom, https://orcid.org/0000-0002-0866-8246 (JCI)

*Corresponding author: aburky@princeton.edu

$$y(t) = \mathcal{L}^{-1}\{Y(s)\} = \mathcal{L}^{-1}\{X(s)H(s)\}, \tag{2}$$

in which $Y(s) = \mathcal{L}\{y(t)\}$, $X(s) = \mathcal{L}\{x(t)\}$, $H(s) = \mathcal{L}\{h(t)\}$, $\mathcal{L}$ represents the Laplace transform,

$$X(s) = \mathcal{L}\{x(t)\} = \int_0^\infty x(t)e^{-st}dt, \tag{3}$$

with $\mathcal{L}^{-1}$ its inverse, and $s = \sigma + i\omega$ is a complex number, with angular frequency $\omega = 2\pi f$, in which f is the common frequency (in hertz). In the transformed space, the Laplace domain, $H(s)$ is called the transfer function. The equivalent (though not identical) quantity in the Fourier domain is the complex frequency response (Wielandt, 2012).

The transfer function can be represented as the ratio of two complex-valued polynomials (Scherbaum, 2001),

$$H(s) = k\frac{(s-z_1)(s-z_2)\ldots(s-z_m)}{(s-p_1)(s-p_2)\ldots(s-p_n)}, \tag{4}$$

with zeros z_i, $i = 1, \ldots, m$, and poles p_i, $i = 1, \ldots, n$, and a gain of k. Therefore, knowledge of the poles, zeros, and gain of the seismometer allows us to construct the transfer function and successfully remove it from the seismogram.

If we rearrange equation (2), we can solve for $x(t)$ as

$$x(t) = \mathcal{L}^{-1}\left\{\frac{Y(s)}{H(s)}\right\}. \tag{5}$$

This reduces our problem of solving for the ground motion $x(t)$ to a division of the Laplace (or Fourier) transform of the seismogram by the instrument's transfer function (or the complex frequency response), which is simple in theory but requires care in practice. It is worth noting that in the preceding discussion, we have been working within the framework of continuous variables and infinite time. In practice, seismograms are finite-time, discretized time series, and all of the aforementioned operations are replaced by their discrete counterparts, accompanied by appropriate preprocessing steps, including demeaning, detrending, and treatment of the edges (e.g., tapering, zero padding).

The Transfer Function

Transfer functions are made publicly available for all broadband digital seismometers deployed by the major seismological research consortia (e.g., Incorporated Research Institutions for Seismology [IRIS], Global Seismographic Network, GEOSCOPE). In practice, the information is typically stored in the form of a `RESP` or a `SAC_PZ` file, but the critical information we need to correct the signal for the instrument response are the poles, the zeros, and the gain constant of the system.

As a complex-valued function, the transfer function can be difficult to visualize and comprehend. Fortunately, the effect of the transfer function on the amplitude and phase of an input signal can be extracted to help us gain a better understanding of what it represents.

The amplitude response of the system can be calculated by taking the absolute value of the transfer function using the following equation:

$$|H| = \sqrt{\mathrm{Re}(H)^2 + \mathrm{Im}(H)^2}. \tag{6}$$

Geometrically, this is the length of the complex-valued H, given by the square root of the sum of the squares of its real and imaginary parts.

The phase response of the system is calculated by finding the argument of the transfer function using the following equation:

$$\mathrm{Arg}\{H\} = \mathrm{atan2}\{\mathrm{Im}(H), \mathrm{Re}(H)\}. \tag{7}$$

Geometrically, this is the angle that the complex-valued H makes with the real axis, given by the arctangent of the ratio between its imaginary and real parts.

Figure 1 shows examples of the amplitude and phase responses, as a function of frequency f, for the vertical component of a Raspberry Shake 3D (R36A4.00), two Nanometrics Trillium Compact 120s seismometers (S0001.00 and S0002.00), and a Nanometrics Titan 1g accelerometer (S0002.10). All of these sensors were operating in Princeton, New Jersey, at the time of the 9 September 2020 M_b 3.1 earthquake in Marlboro, New Jersey. We note that these responses have different yet related shapes for different choices of output units. This is because each of these response curves differs by a factor of $i\omega$ and thus corresponds to successive rotations of the frequency response by $2\pi f$. Most broadband seismometers have a portion of their amplitude response that is flat in velocity, as can be seen for the Raspberry Shake 3D and the Trillium Compact 120s (Fig. 1c). The Titan 1g has a flat response to acceleration (Fig. 1e).

It is important to keep in mind how gain and phase vary as a function of frequency because this affects the outcome of the eventual instrument response removal by deconvolution or spectral division as we discuss next. However implemented, undoing the system response by converting a record from one of the Trillium Compact 120s seismometers to velocity amplifies the output at periods >100 s (<0.01 Hz), whereas performing the same operation on the Raspberry Shake 3D greatly amplifies the output at periods >1 s (<1 Hz). Although the proper removal of the instrument response ensures that the frequency-dependent shape of the instrumental transfer function is accounted for, signal-to-noise considerations will dictate whether the original output at those periods can be trusted, or indeed, is of any interest.

These considerations illustrate the need for a judicious application of prefiltering prior to instrument response removal. A prefilter removing only periods longer than about 100 s might be fine for the Trillium Compact 120s but would be an inappropriate choice for the Raspberry Shake 3D, which is not designed to record signals at such a long period.

SAC Implementation

Before continuing to our example of removing the instrument response, we briefly review the existing Seismic Analysis Code (SAC) algorithms that do so (Goldstein and Snoke, 2005). As mentioned previously, the instrument response information typically comes as a `RESP` file or a `SAC_PZ` file. SAC provides functionality for removing either response specification using the `transfer` function, and although the results are nearly indistinguishable, there are minor differences in the algorithms that are worth commenting on. The essential problem solved by both algorithms is: given poles, zeros, and gain, construct the transfer function and deconvolve it from the seismogram of interest.

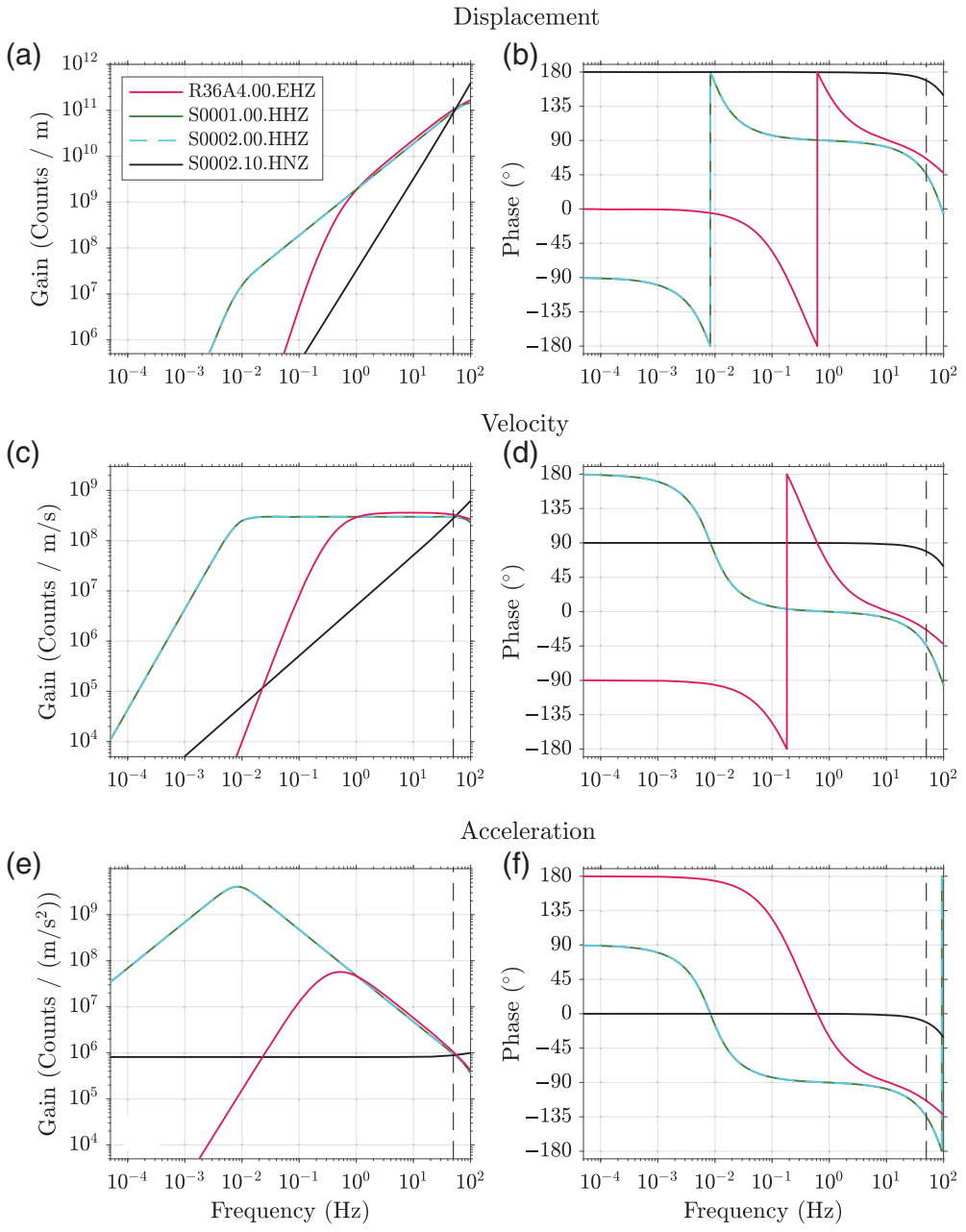

Figure 1. (a,b) Displacement, (c,d) velocity, and (e,f) acceleration amplitude and phase responses of a variety of instruments that recorded the Marlboro, New Jersey, earthquake in 2020. The Nyquist frequency of each instrument is indicated by the dashed vertical line at 50 Hz. Note that the amplitude responses to velocity of the Nanometrics Trillium Compact 120s seismometers and the Raspberry Shake 3D are flat, as is the response to acceleration of the Titan 1*g* accelerometer.

The main difference between the two algorithms is in the first step: the construction of the transfer function. When SAC `transfer` is called with a `RESP` file, it calls `evalresp`, an external C program, which constructs the transfer function with a length equal to that of the data vector. The call is restricted to returning a transfer function with no more than $2^{16} = 65,536$ points, and in the event that the data vector is longer, the transfer function is interpolated to match the length of the data vector. In contrast, when SAC removes the instrument response using a `SAC_PZ` file, it internally constructs the transfer function from the poles, zeros, and gain constant, with a length equal to that of the data vector rounded to the next power of 2, with no upper bound on the number of samples. After this, in both cases, the discrete Fourier transform of the zero-padded seismogram of interest is taken, the prefilter is applied, and that frequency representation is divided by the (interpolated) frequency response function. SAC then takes an inverse discrete Fourier transform of the data to return to the time domain. The difference between these two methods is often subtle but sometimes noticeable.

Open-Source Implementation: `rflexa`

As a means of practically introducing these concepts to researchers and students of seismology, we have incorporated an instructional module as part of our `rflexa` software package. This module is available in both MATLAB and Python to accommodate a wider range of programming backgrounds. The key elements of the module are downloading seismic data and requesting and saving the instrument response information (in the `RESP` or `SAC_PZ` file format, or both), parsing the response to construct the transfer function, visualizing the transfer function, and removing the transfer function (correcting for the instrument response). We hope that this will serve as a useful starting point for new and experienced students of seismology.

To briefly showcase some of `rflexa's` functionality, we examine data from the M_{Lg} 3.1 earthquake in Marlboro, New Jersey (Fig. 2). Four different instruments recorded this event in Princeton, New Jersey: a Raspberry Shake 3D, located ~5 m above ground level in university student housing (Fig. 2a), and two Trillium Compact 120s seismometers and a Titan 1*g* accelerometer, all located in the basement of the Geosciences Department Guyot Hall (Fig. 2b,c). The earthquake occurred roughly due east of Princeton at an epicentral distance of 31.4 km, and the motion recorded on each instrument was of a similar order of magnitude despite the different response characteristics of each sensor. To appropriately compare the records on each instrument, however, we ought to convert each record to a consistent physical unit (displacement, velocity, or acceleration). To obtain the results shown in Figure 3, we used the `transfer` function of the `rflexa` library, which was benchmarked against the SAC function of the same name (Fig. 4).

To call `transfer`, we need a vector of equally spaced (preprocessed) data; their sampling interval; a vector of four frequencies that define the corners of a cosine filter applied to the data before deconvolving the instrument response; and three strings that specify the desired output type, the path to the file containing the instrument response information, and a flag indicating whether that file is of type `SAC_PZ` or `RESP`. The function returns the appropriate ground motion. An example of the syntax used to call the function in MATLAB to produce the velocity records in Figure 3 is:

```
freqLims = [0.1, 0.2, 10, 20];
groundmotion = transfer(instrumentcounts,…
  deltat,freqLims,'velocity'…,
  'pzFile','sacpz');
```

After successfully calling `transfer` and removing the instrument response from the records shown in Figure 2, we observe that the shapes of the waveforms shown in Figure 3 are quite similar. One can even see coherent arrivals in the *P*-wave coda on all four instruments. In addition, the amplitude of the velocity is roughly the same for each instrument. This example highlights the importance of correctly accounting for the instrument response as a preliminary step in the analysis of seismic data because we can now compare all of our records consistently. With the ever increasing quantity and diversity of seismic instruments (Anthony *et al.*, 2019; Simon *et al.*, 2021), properly correcting for the instrument response remains as significant as ever.

In addition to providing functionality for removing the instrument response, `rflexa` provides a function that allows for the quick visualization of the instrument response contained in a `SAC_PZ` or `RESP` file. This function, `bodePlot`, which takes its name from the electrical engineering and control theory literature, takes two inputs, corresponding to the last two inputs to `transfer` defined previously. An example of this function's syntax, by which we generated the panels in Figure 1, is

```
bodePlot(pzFile,'sacpz');
```

We hope and expect that this function might prove useful as researchers consider the sensitivity of the instruments they are using before choosing prefiltering corner frequencies. Both of these functions and their dependencies have analogous versions in Python. Also included are helper functions to save and parse `SAC_PZ` and `RESP` files in both languages.

The 2020 Marlboro Earthquake

Before concluding, it is worth commenting on the earthquake itself, given that seismicity is so uncommon in New Jersey and the rest of the northeastern United States. Some authors have proposed that seismicity in the northeast may not be characterized by a Poissonian distribution (Ebel and Kafka, 2002), suggesting that rare events such as this ought to be paid attention to as potential indicators of periods of enhanced seismicity. From a cultural perspective, this earthquake was reported as having been felt by >7000 individuals and reported to the U.S. Geological Survey's "Did You Feel It?" (Wald *et al.*, 2012) service, which is unsurprising given the high-population density of the New Jersey–New York metropolitan area. Geologically speaking, the earthquake occurred near the boundary of the Vincentown–Hornerstown Formation, of Paleocene age and the Tinton–Red Bank Formation of upper Cretaceous age (Owens *et al.*, 1995). Both of these units are composed of quartz sand, with the Vincentown–Hornerstown Formation additionally containing coquina and bryozoan reef deposits. The nearest mapped fault in the region is the Ramapo fault, which trends northeast–southwest ~50 km to the northwest of the epicenter of the Marlboro earthquake. Scattered seismicity has occurred near this fault in recent times (Page *et al.*, 1968), but the general pattern of seismicity in the greater New York City area does not show clear concentration along the Ramapo or any other mapped fault (Kafka *et al.*, 1985, 1989). Thus, the cause of the Marlboro earthquake remains enigmatic.

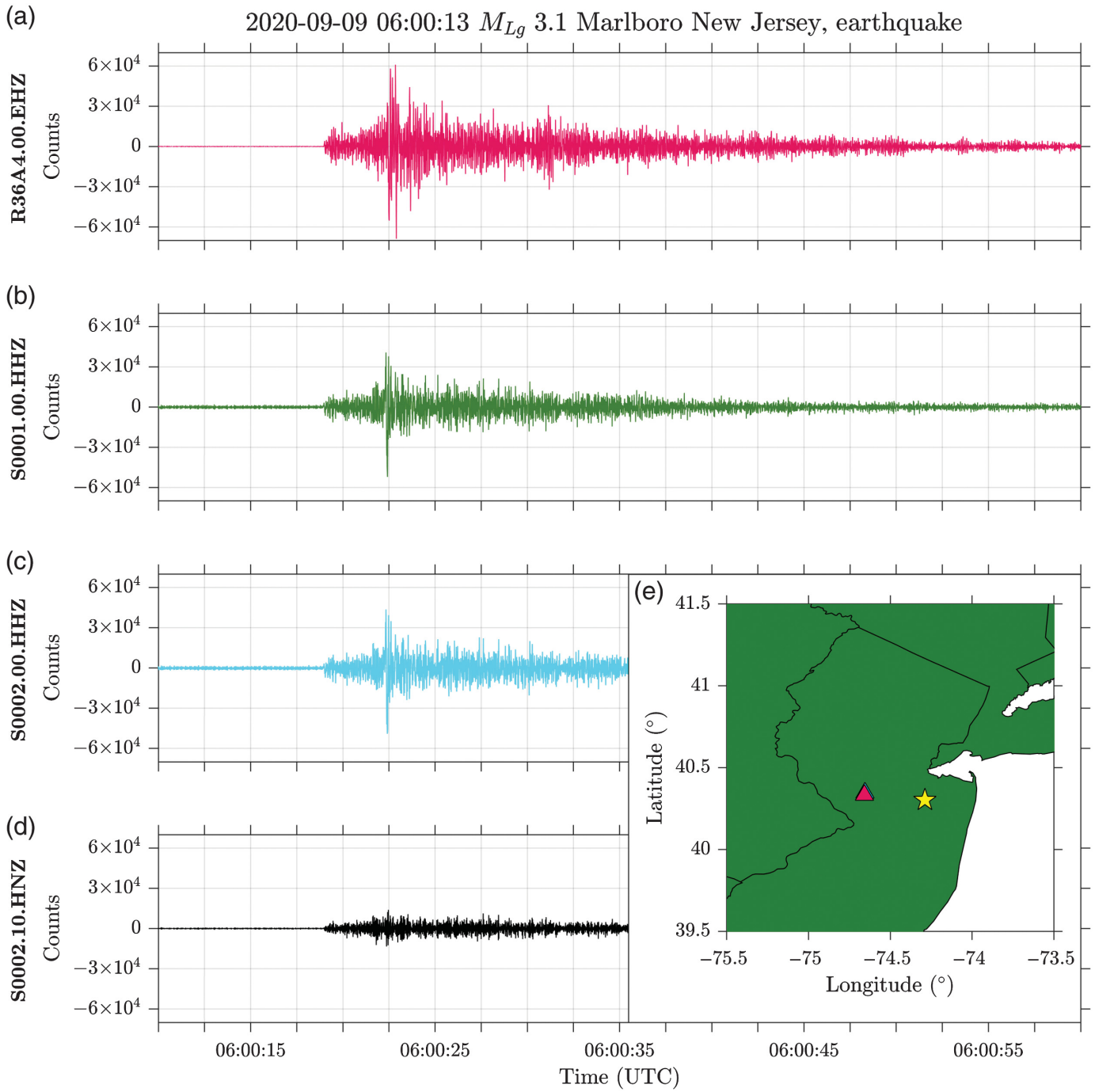

Figure 2. Unprocessed vertical-component records of the 9 September 2020 M_{Lg} 3.1 Marlboro, New Jersey, earthquake from four different instruments: (a) a Raspberry Shake 3D, (b) a Trillium Compact 120s, (c) a Trillium Compact 120s (part of a Trillium Cascadia), and (d) a Titan 1*g* accelerometer (also part of the Trillium Cascadia), all located in Princeton, New Jersey. (e) The location of the instruments (triangles) relative to the earthquake (star). Note that all records are in digital counts. Instruments (b), (c), and (d), are located within 0.5 m of one another in the basement of a building on campus, and instrument (a) is located ~5 m above ground level in a two-story university student housing building. The U.S. Geological Survey National Earthquake Information Center reported a location of 40.302° N 74.289° W and a depth of 5.6 km for this event.

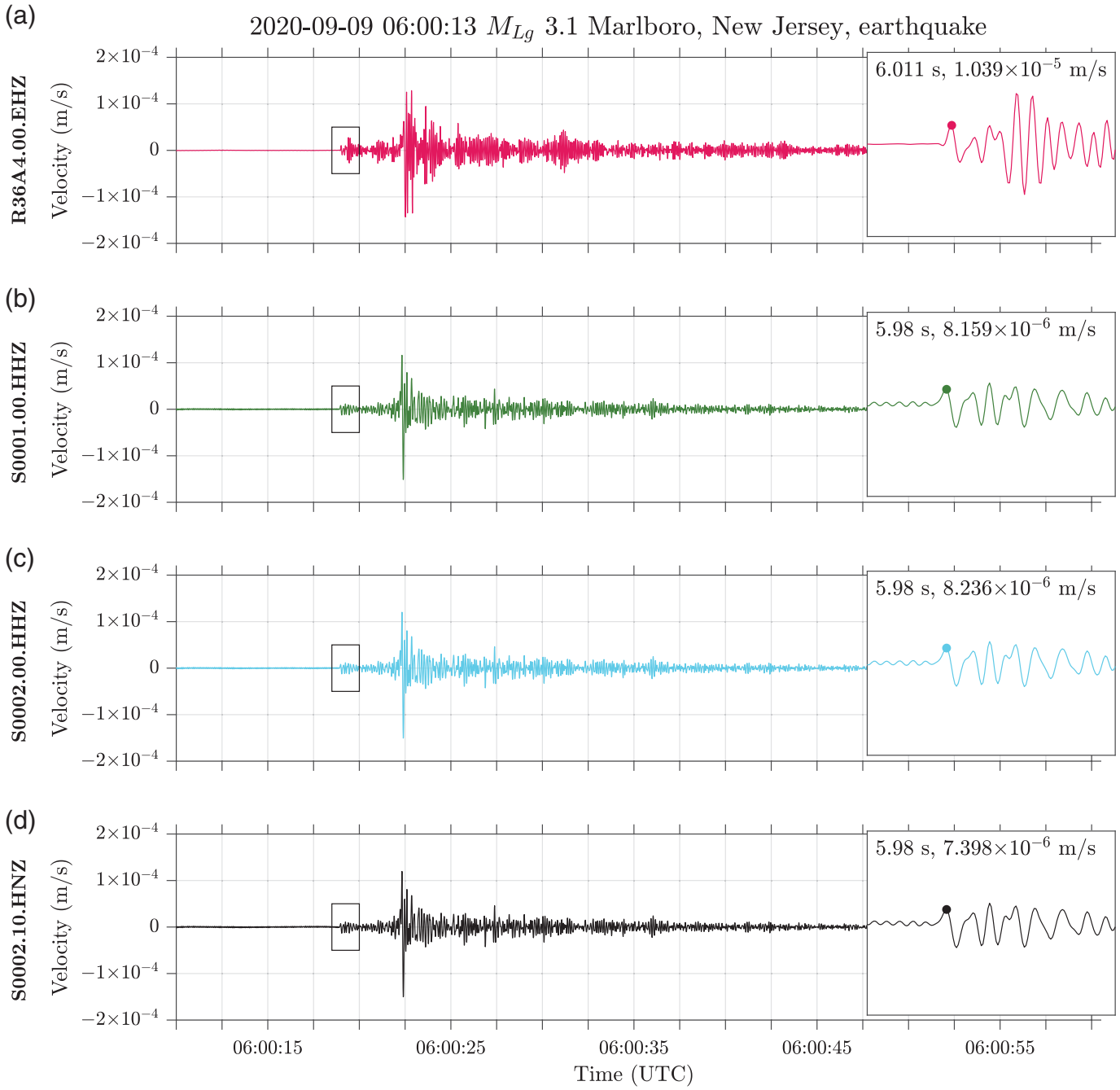

Conclusion

We have reviewed the physical motivation for, and some mathematical theory behind, the removal of the instrument response from digital seismic records. After outlining the practical details of acquiring and accounting for the instrument response, we discussed appropriate use cases and considerations. We then presented open-source routines in MATLAB and Python that perform the instrument response removal and provided functions for visualizing transfer functions. Finally, we presented examples from four different instruments of records of the M_b 3.1 Marlboro, New Jersey, earthquake as a

Figure 3. (a–d) The seismograms of Figure 2 after band-pass filtering between 0.2 and 10 Hz and removing the instrument response to convert the records to velocity. Note that the amplitude of motion recorded on each instrument is approximately equal. The first motions, corresponding to the *P*-wave arrival, recorded by each instrument are emphasized in the zoomed-in sections. Perhaps surprisingly, the Raspberry Shake 3D in (a) has the least pre-event noise of all of the instruments shown. Annotations in the inset panels provide the arrival time and amplitude of the maximum of the first arriving pulse, marked by a filled circle.

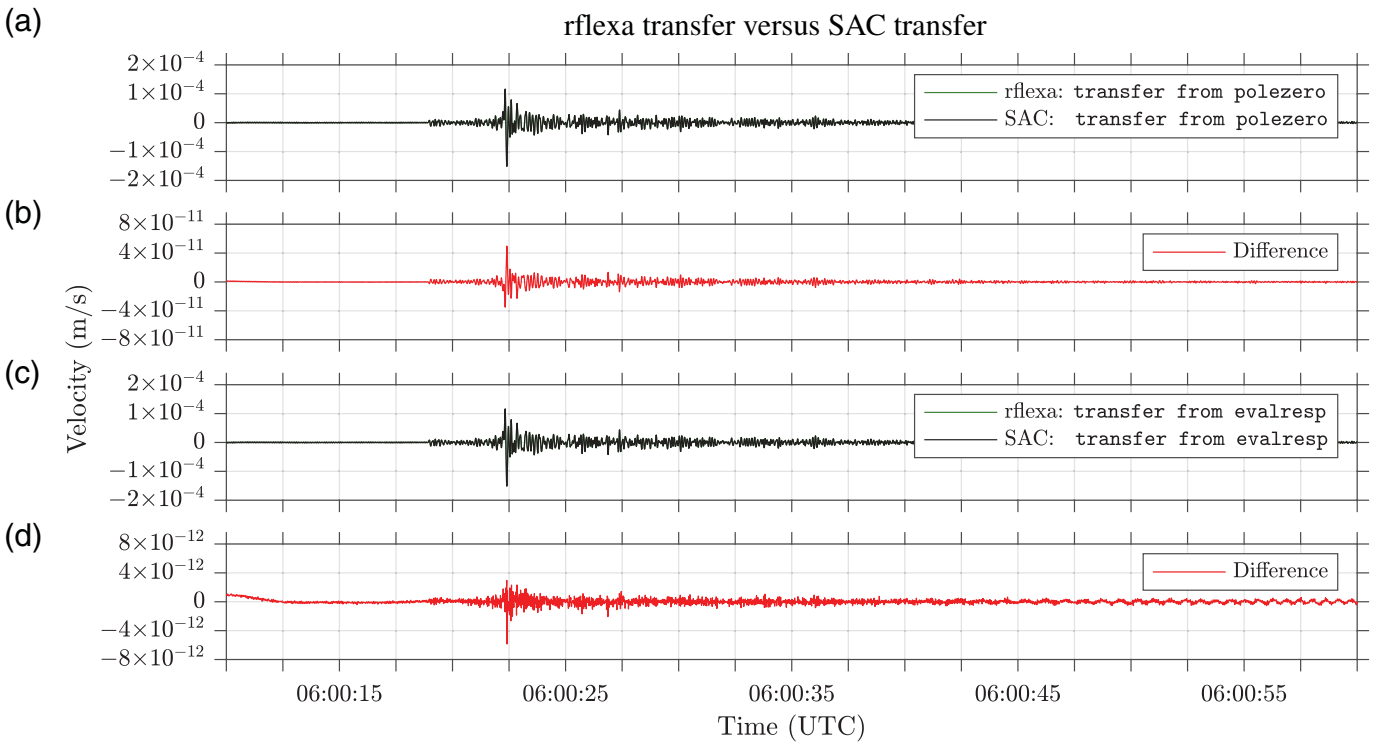

Figure 4. Comparison of instrument response removal methods. (a) Record after instrument response removal using the `transfer` from polezero… syntax in Seismic Analysis Code (SAC) and the record converted using the analogous command in our open-source package, `rflexa`. (b) Difference (in red) between the two records in (a). (c) Records after instrument-response removal using the `transfer` from evalresp… syntax in SAC. (d) Difference (in red) between the two records in (c). The differences between the results are on the order of machine precision, verifying that the algorithms are benchmarked acceptably.

concrete illustration of instrument response removal in practice for a rare earthquake in our home state. Interested readers can find the code, tutorials, animations, and instructional modules in the Data and Resources.

Data and Resources

Seismograms used in this study were recorded using instruments on or near Princeton University and are available with their corresponding instrument response data at https://github.com/alexburky/rflexa/tree/master/transfer/data. In addition, the Raspberry Shake 3D data are available for download online from the Incorporated Research Institutions for Seismology Data Management Center (IRIS-DMC) at www.iris.edu. We have also made use of the Seismic Analysis Code (SAC) software package, which can be requested at http://ds.iris.edu/ds/nodes/dmc/forms/sac/, and Matlab version R2020b which can be accessed at http://www.mathworks.com/products/matlab. All websites were last accessed in July 2021.

Declaration of Competing Interests

The authors acknowledge there are no conflicts of interest recorded.

Acknowledgments

The authors thank the Incorporated Research Institutions for Seismology (IRIS) for providing the Seismic Analysis Code (SAC) software package (and its source code) to use as a reference for benchmarking our codes. Partial support for this work was provided by the National Science Foundation (NSF) under Grant Number EAR-1736046. The authors thank Lucas Sawade for providing access to the Raspberry Shake 3D data, and the authors also thank the Princeton Department of Geosciences, the High Meadows Environmental Institute, and the Freshman Seminar Program for acquiring the instrumentation. The authors are grateful to Alan Kafka for contributing his insight and Adam Ringler for a detailed and constructive review.

References

Anthony, R. E., A. T. Ringler, D. C. Wilson, and E. Wolin (2019). Do low-cost seismographs perform well enough for your network? An overview of laboratory tests and field observations of the OSOP Raspberry Shake 4D, *Seismol. Res. Lett.* **90,** no. 1, 219–228, doi: 10.1785/0220180251.

Asch, G. (2009). Seismic systems, in *New Manual of Seismological Observatory Practice 2 (NMSOP-2)*, P. Bormann (Editor), Deutsches GeoForschungsZentrum, IASPEI, Potsdam, Germany, Chapter 6, 1–20, doi: 10.2312/GFZ.NMSOPr1 ch6.

Bormann, P. (Editor) (2012). *New Manual of Seismological Observatory Practice 2 (NMSOP-2)*, Deutsches GeoForschungsZentrum, IASPEI, Potsdam, Germany.

Ebel, J. E., and A. L. Kafka (2002). A non-Poissonian element in the seismicity of the northeastern United States, *Bull. Seismol. Soc. Am.* **92,** no. 5, 2040–2046, doi: 10.1785/0120010211.

Goldstein, P., and A. Snoke (2005). SAC availability for the IRIS community, *Incorp. Res. Inst. Seismol. Newsl.* **7,** UCRL-JRNL-211140, https://www.osti.gov/servlets/purl/875360 (last accessed July 2020).

Havskov, J., and G. Alguacil (2016). *Instrumentation in Earthquake Seismology*, Springer, Heidelberg, Germany.

Kafka, A. L., E. A. Schlesinger-Miller, and N. L. Barstow (1985). Earthquake activity in the greater New York City area: Magnitudes, seismicity, and geologic structures, *Bull. Seismol. Soc. Am.* **75,** no. 5, 1285–1300.

Kafka, A. L., M. A. Winslow, and N. L. Barstow (1989). Earthquake activity in the greater new york city area: A fault finder's guide, *Field Trip Guidebook, 61st Annual Meeting, New York State Geological Association*, 177–205.

Owens, J. P., P. J. Sugarman, N. F. Sohl, R. Parker, H. H. Houghton, R. V. Volkert, A. A. Drake, and R. C. Orndorff (1995). Geologic map of New Jersey: Central Sheet, scale 1:100,000, *U.S. Geol. Surv. Open-File Rept. 95-253*, U.S. Department of the Interior, Geological Survey.

Page, R. A., P. H. Molnar, and J. Oliver (1968). Seismicity in the vicinity of the Ramapo fault, New Jersey-New York, *Bull. Seismol. Soc. Am.* **58,** no. 2, 681–687.

Ringler, A. T., and P. Bastien (2020). A brief introduction to seismic instrumentation: Where does my data come from? *Seismol. Res. Lett.* **91,** no. 2A, 1074–1083, doi: 10.1785/0220190214.

Scherbaum, F. (2001). Of Poles and Zeros: Fundamentals of Digital Seismology, Second Ed., Kluwer, Norwell, Massachusetts.

Simon, J. D., F. J. Simons, and J. C. E. Irving (2021). A MERMAID miscellany: Seismoacoustic signals beyond the *P* wave, *Seismol. Res. Lett.* 1–11, doi: 10.1785/022021005.

Wald, D. J., V. Quitoriano, C. B. Worden, M. Hopper, and J. W. Dewey (2012). USGS "Did You Feel It?" Internet-based macroseismic intensity maps, *Ann. Geophys.* **54,** no. 6, 688–707, doi: 10.4401/ag–5354.

Wielandt, E. (2012). Seismic sensors and their calibration, in *New Manual of Seismological Observatory Practice 2 (NMSOP-2)*, P. Bormann (Editor), Deutsches GeoForschungsZentrum, IASPEI, Potsdam, Germany, Chapter 5, 1–51, doi: 10.2312/GFZ.NMSOP–2_ch5.

Manuscript received 7 May 2021